Solvent-Free Synthesis of Co-Based Zeolitic Imidazolate Framework (ZIF-9) for the Removal of Congo Red from Water

Khoa Dang Tran[1,2], Hoan Tuan Phan[1,2], Chi Thi Kim Nguyen[1,2], Bao Chi Nguyen[1,2], Ha Vu Le[1,2], and Khoa Dang Nguyen[1,2*]

[1]*Faculty of Chemical Engineering, Ho Chi Minh City University of Technology (HCMUT), 268 Ly Thuong Kiet Street, District 10, Ho Chi Minh City 740010, Vietnam*

[2]*Vietnam National University Ho Chi Minh City, Linh Trung Ward, Thu Duc District, Ho Chi Minh City 720325, Vietnam*

* ***Corresponding author:***

tel: +84-838647256
email: khoand1989@hcmut.edu.vn

Received: August 14, 2024
Accepted: November 19, 2024

DOI: 10.22146/ijc.99141

Abstract: *The study presented a green and benign approach via mechanochemistry for rapidly preparing a typical cobalt-based zeolitic imidazolate framework, namely ZIF-9. The structural, morphological and textural properties of the obtained material were confirmed by X-ray diffraction (XRD), scanning electron microscopy (SEM), and nitrogen sorption at 77 K. The prepared material was then employed as an efficient adsorbent to remove Congo red (CR) from the aqueous solution. Intensive experiments were then conducted with the removal of CR to investigate the effect of adsorption conditions, including contacting time, pH value, and initial concentration of organic dye solution. The adsorption process follows the pseudo-second-order kinetic model, indicating that the adsorption of the CR dye is primarily chemical adsorption. The Langmuir model fitted the experimental data with a maximum adsorption quantity of 248.22 mg/g. Besides, the adsorption capacity of prepared ZIF-9 still remained stable after three cycles. This strategy was a simple method compared to conventional methods in terms of reducing the amount of used solvents, energy requirements, and the duration of the synthetic process.*

Keywords: *mechanochemistry; ZIF-9; zeolitic imidazolate frameworks; Congo red; adsorption*

■ INTRODUCTION

With rapid industrialization and inefficiently planned urbanization, the excessive discharge of effluents containing organic dyes has not only severely threatened public health but also caused environmental deterioration due to their low biodegradability and the potential source of carcinogenicity [1-3]. Congo red (CR) is a typical example of an anionic azo dye that is widely used. These dye molecules pose significant health risks, causing allergies and diseases affecting the eyes, skin, respiratory system, reproductive system, and even leading to cancer and genetic mutations [3]. However, due to their low cost and desirable properties, such as high durability under standard production and storage conditions, brighter colors, etc., azo dyes continue to be used [4]. Hence, the treatment of water contaminated by CR is crucial.

Numerous treatments have been utilized for dye removal, namely membrane filtration, irradiation, advanced oxidation processes, electrochemical degradation, ozonation [5-6] and photodegradation [7-8]. Some of the key aspects inhibiting their scope of application lie in their affordability and need for specialized equipment. Therefore, adsorption has been deemed promising in water decontamination due to process simplicity, cost-effectiveness, potential of regeneration and lack of secondary pollution, in which the exploration of the fabrication of proper adsorbents is tremendously centralized [5,9]. More research has been carried out to study the adsorption ability of various adsorbents for removing CR dye in wastewater [10-12].

A prominent class of porous material, namely metal-organic frameworks (MOFs), has recently drawn tremendous attention from many scientists. The

particular interest in MOF materials is in the light of the possible modification of their pore size and high surface area [13-14]. It should be noted that for MOFs to be employed in water purification, substantial water stability is a prerequisite, in which zeolitic imidazolate frameworks (ZIFs), a subclass of MOFs, are reported to be an outstanding candidate [14-15]. In ZIFs, the carboxylic acid linkers are replaced by imidazole linkers, and the metal-oxygen bonds are replaced by metal-nitrogen bonds, thus enhancing the bond's stability compared to MOFs. Particularly, ZIF-9 is constructed from tetrahedral cobalt ions bridged by benzimidazolate, forming the extended crystalline three-dimensional network [16-17]. Although the pore diameter of ZIF-9 was quite small, about 0.29 × 0.43 nm, the external surface of the structure could strongly bind to organic compounds or dye molecules via aromatic π-π stacking, electrostatic and coordination bonding [16,18-19]. This material was also reported to be a typical hydrophobic material, which is tremendously advantageous for the efficient capture of organic molecules. Therefore, ZIF-9 can be deemed a promising material for treating wastewater containing organic substances [20].

In previous studies, ZIF-9 material was commonly synthesized using solvothermal methods with solvents like DMF. However, expensive organic solvents that are flammable and environmentally unfriendly have limited the application of this material in environmental treatment due to their negative impact on the environment and living organisms. Mechanochemistry has proven highly effective for synthesizing MOFs and other metal-organic materials. Short reaction times and quantitative conversion, coupled with lack of solvent, allow mechanochemistry to provide MOFs faster and simpler than conventional routes [21]. These techniques have facilitated the rapid and efficient assembly of nearly all major MOF families, including MOF-5, ZIFs, UiO-66 systems, and HKUST-1 [22-24]. Therefore, in this study, ZIF-9 was prepared facially via free-solvent mechanochemistry towards the application for the removal of Congo red from water, in which the stoichiometric metal-ligand was applied. The adsorption behavior of ZIF-9 was explored for CR under varied conditions, including contact time, initial concentration, and pH. The isothermal and kinetics models of the CR adsorption were also discussed in this work.

■ EXPERIMENTAL SECTION

Materials

Chemicals in this study were purchased from commercial suppliers (Xilong, Merch, Acros) and used directly without any further purification. Cobalt nitrate hexahydrate ($Co(NO_3)_2{\cdot}6H_2O$, 98%, Xilong), benzimidazole (bIm, 99%, Merch), and potassium carbonate (K_2CO_3, > 99%, Acros) were used as precursors for ZIF-9 synthesis. CR dye (98%) used for the adsorption experiments was purchased from Xilong.

Instrumentation

Scanning electron microscopy (SEM) studies were conducted on a S-4000 microscope (Hitachi, Japan). The N_2 adsorption-desorption isotherm was measured at liquid nitrogen temperature 77 K after vacuum activation at 120 °C overnight and the surface area was calculated by the Brunauer–Emmett–Teller (BET) method. Powder X-ray diffraction (PXRD) patterns were recorded between 5° and 50° using a CuKα radiation source on a D8 Advance Bruker.

Procedure

Preparation of zeolitic imidazolate framework material, ZIF-9

In a typical preparation, 0.44 g of $Co(NO_3)_2{\cdot}6H_2O$ (1.50 mmol), 0.35 g of bIm (3.00 mmol) and 0.21 g of K_2CO_3 (1.50 mmol) were ground thoroughly for 60 min at ambient condition. The resulting mixture color was purple. The sample was then washed by centrifugation with 3 × 30 mL H_2O and 3 × 30 mL acetone to remove water-soluble substances and excess starting reagents. Subsequently, the material was soaked in acetone for 3 d and dried under vacuum at 120 °C for 4 h, affording activated samples for experiments.

Adsorption studies

To evaluate the adsorption capacity, the as-prepared ZIF-9 was added to 15 mL of CR solution with an initial concentration of 100 ppm in a 20 mL vial with

a cap. The experiment was conducted at room temperature (~30 °C) with continuous stirring for 4 h. Afterwards, the clean supernatant was collected via centrifugation (3000 rpm, 5 min). The concentration of CR was determined with a UV–vis spectrophotometer (Thermo Scientific G10S) at λ = 497 nm and subsequently calculated via the analytical calibration curve. The effect of experimental parameters on the CR capture of ZIF-9, including adsorption time (0–360 min), initial CR solutions (50–1000 ppm), and initial pH (4–11), were investigated. After each experiment, Eq. (1) was employed to calculate the equilibrium adsorption capacity (q_e, mg/g) of the ZIF-9 material;

$$q_e = \frac{C_0 - C_e}{m} V \quad (1)$$

where C_0 is the initial concentration of the CR solution (mg/L), C_e is the concentration of CR at equilibrium (mg/L), V is the volume of CR solution (L), m is the mass of ZIF-9 (g).

Based on the profile of the time-dependent adsorption, two models, namely, pseudo-first-order (Eq. (2)) and pseudo-second-order (Eq. (3)) models were employed to clarify the interaction of CR molecules and ZIF-9 external surface [25-26].

$$\ln(q_e - q_t) = \ln q_e - k_1 t \quad (2)$$

$$\frac{t}{q_t} = \frac{1}{k_2 q_e^2} + \frac{1}{q_e} t \quad (3)$$

The theoretical Langmuir (Eq. (4)) and Freundlich isotherm equations (Eq. (5)) in the linearized form were employed to investigate the adsorption model of Congo red molecules and ZIF-9 material [27-28];

$$\frac{1}{q_e} = \frac{1}{q_m K_L C_e} + \frac{1}{q_m} \quad (4)$$

$$\ln(q_e) = \frac{1}{n} \ln C_e + \ln K_F \quad (5)$$

where q_m is the maximum amount of adsorption (mg/g), K_L is the Langmuir constant related to the energy of adsorption, K_F and n are Freundlich constants.

■ RESULTS AND DISCUSSION

The crystalline phase of the as-prepared sample was investigated by XRD. As expected, the patterns of the as-synthesized ZIF-9 showed a good agreement with the simulated structure of ZIF-9. Particularly, it was observed that XRD results exhibited signature peaks at 2θ = 6.97, 7.57 and 9.10° (Fig. 1), corresponding to the crystalline phase of ZIF-9. These obtained signals were consistent with previous reports, indicating that ZIF-9 was successfully synthesized via mechanochemistry [29-30]. It should be noted that ZIF-9 fabrication relied on the presence of basic compounds to promote the production of benzimidazolate bridges.

Insufficient basicity hindered the deprotonation of benzimidazole ligands, resulting in prolonged synthesis duration. In contrast, the excessively basic inorganic salt inhibited the desired formation of the highly crystalline ZIF-9 phase. Therefore, the selection of substances with appropriate basicity is critical for an efficient and high-quality ZIF-9 synthesis. Within this study, the utilization of K_2CO_3 as a basic salt for the successful synthesis of ZIF-9 was necessary, proving the feasibility of successful synthesis of the crystalline phase of ZIF-9 with K_2CO_3, deviating from the previously reported employment of $NaHCO_3$ [29]. In addition, employing such procedures reduced reaction time and eliminated the utilization of solvents, thus providing a facial and solvent-free approach to ZIF-9 fabrication.

Nitrogen isothermal sorption measurements were carried out to evaluate the textural properties of ZIF-9. The low-pressure nitrogen uptake confirmed the presence of microporosity. The higher slope at the intermediate pressure region suggested an increasing accumulation of

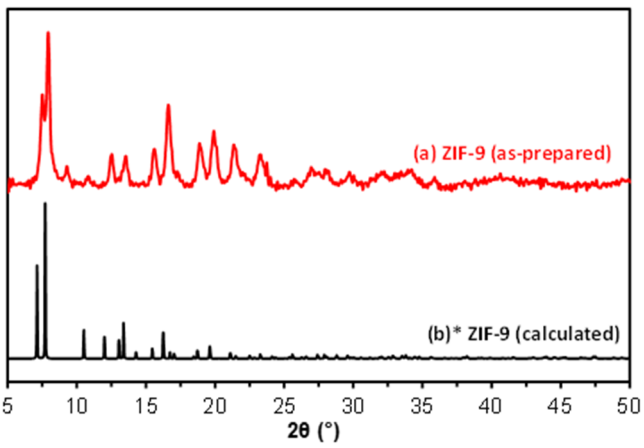

Fig 1. PXRD pattern of (a) as-prepared ZIF-9 and (b) calculated ZIF-9 [31]

non-microporosity, accompanied with the hysteresis at intermediate pressure regions ($p/p_0 > 0.4$), which indicated capillary condensation [32]. The obtained isotherm revealed that no maximum quantity adsorbed in the relative pressure range greater than 0.97 was achieved, confirming the presence of a broad range of pores consisting of micro-, meso-, and macro-pores in as-prepared ZIF-9. Indeed, DFT-derived calculations demonstrated a large distribution of pore sizes, including 1.72, 2.34, and 50.40 nm (Fig. 2). Moreover, the BET-specific surface area was calculated to be 5.43 m^2/g, which was well-aligned with previous reports due to the low nitrogen uptake [30]. It could be rationalized that the pore diameter of the material was far smaller than the kinetic diameter of nitrogen molecules to afford a high uptake of nitrogen during the analysis.

The morphology and structural characteristics of the as-synthesized ZIF-9 were investigated via SEM (Fig. 3). The SEM images revealed two distinct morphologies consisting of stacked sheet-like layers and almost cube shapes with irregular distribution. This observation suggested a possible incomplete crystal growth process, with a chemical transformation from a cube shape towards a sheet-like structure, suggesting an influence of water content during ZIF-9 synthesis. Initially, limited water molecules might favor the formation of the cubic phase. As the synthesis progressed, the prolonged exposure to water molecules in the air during the fabrication stage likely promoted the sheet-like structure [30]. In agreement with the study of Chen and co-workers [30], increasing the water-to-ethanol ratio was discovered to induce the phase evolution from 3D to 2D ZIF-9. Notably, both recorded morphologies are consistent with previously reported ZIF-9 syntheses *via* solvothermal and hydrothermal methods [30,33-34].

To highlight the application of ZIF-9 prepared by the mechanical route, ZIF-9 was employed to remove CR from the aqueous solution. The adsorption experiments were conducted over intervals ranging from 0 to 360 min to investigate the influence of adsorption

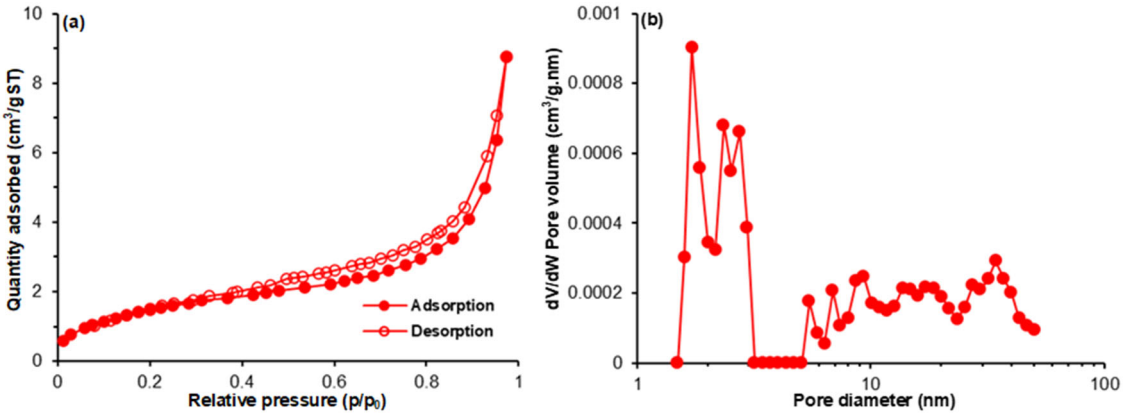

Fig 2. (a) Nitrogen sorption isotherms at 77 K and (b) pore distribution of ZIF-9

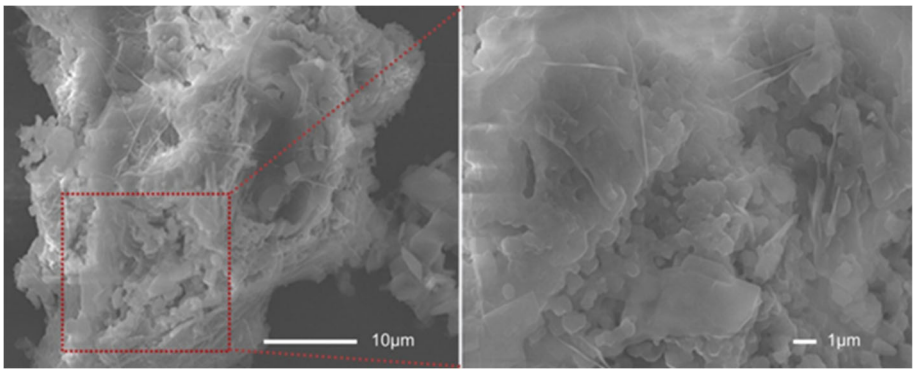

Fig 3. SEM images of as-prepared ZIF-9 with different scales

time, in which 10 mg of ZIF-9 was added into 15 mL CR solution with an initial concentration of 100 ppm. The adsorption of CR occurred rapidly in the initial 5 min, followed by a gradual decline in adsorption rate. The trapping capacity reached approximately 126.0 mg/g within 1 min of adsorption, while this value could rise up to 165.4 mg/g after 60 min, respectively. The removal efficiency reached a saturation state of approximately 200 mg/g after 4 h (Fig. 4), and no further improvement was observed over the extension of time. The uptake trend could be attributed to the abundance availability of binding sites, favoring the quick removal of CR molecules [35]. Once these sites were completely occupied by CR molecules, the adsorption rate became slower, indicating the equilibrium state was acquired. A similar tendency was also observed in the study on the adsorptive removal of MB using ZIF-67 [36].

The time-dependent adsorption results were analyzed using two kinetic models, including pseudo-first-order and pseudo-second-order models (Fig. 5). The coefficient of determination of the pseudo-first-order and pseudo-second-order model (R^2) was 0.8834 and 0.9989, respectively, thus indicating the pseudo-second-order model offered a more appropriate description of the CR adsorption process towards ZIF-9 framework. Additionally, a calculated q_e of 210.86 mg/g closely matched the experimental value ($q_{e,exp}$), suggesting chemical adsorption was mainly responsible for the adsorption mechanism, which was well-aligned with the proposed adsorption concept of ZIF-9 and study of Dai et al. [19]. It should be noted that the rate and trapping capacity of CR removal of as-prepared ZIF-9 was far faster and higher as compared to the modified ZIF-9 toward increasing macroporous volume in Dai and et al. study, in which CR uptake obtained approximately 40 mg/g within 30 min of adsorption process while as-reported ZIF-9 acquired 5 min to afford nearly 120 mg/g, proving the rapid and efficient treatment of CR in water. In other words, the trapping capacity of ZIF-9 possibly exhibited the reliance on the polar surface of ZIF-9, where the formation of various interactions, including electrostatic attraction, π-π interaction and coordination bonding rather than the accessible space.

The positively charged metal centers likely interact favorably with the negatively SO_3^- charged groups of CR

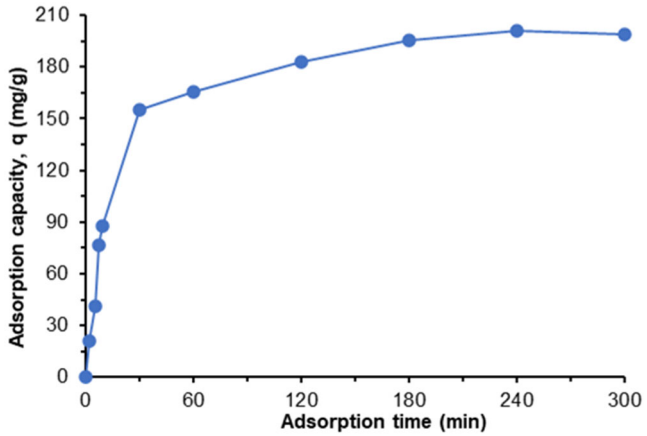

Fig 4. CR uptake versus the adsorption time (Experimental condition: ZIF-9 10 mg, 15 mL CR solution 100 ppm)

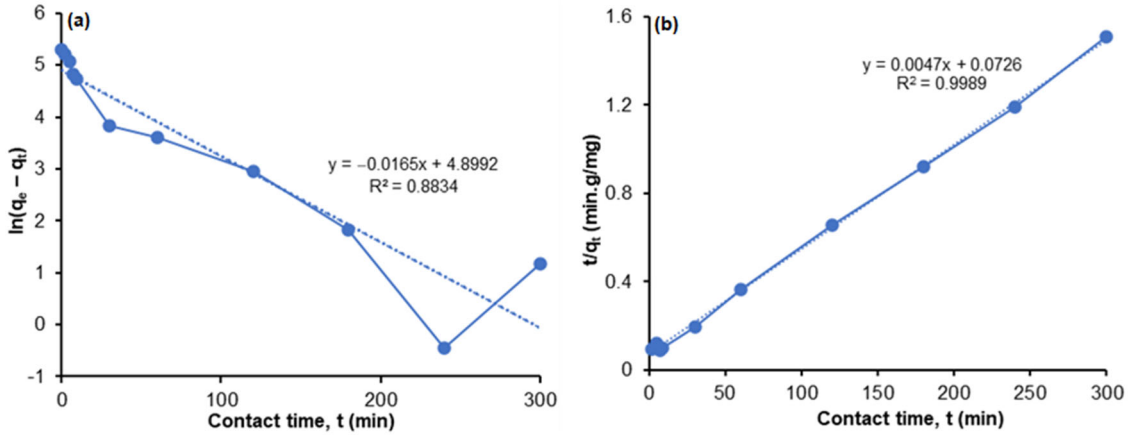

Fig 5. CR adsorption kinetics in (a) first-order and (b) second-order models

molecules via electrostatic attractions. Moreover, π-π stacking between the π-system of the aromatic ring of benzimidazolate ligands and the conjugated aromatic skeleton of CR dyes, along with potential coordination between the nitrogen moieties in bIm and Co^{2+}, further contributed to strong chemical binding between the dye molecules and the ZIF-9 surface (Fig. 6). It should be noted that the accumulative micro- and meso-pore volume of ZIF-9 was determined to account for approximately 93%, whereas the theoretical molecular size of CR is reported to be approximately 1.46 × 0.93 × 2.6 nm, which is too large for organic dye molecules to penetrate the framework. In fact, the inter-particular pores as well as the pores of the outer surface of the particles, might be responsible for capturing the CR molecules, which were observed in the SEM images. The intrinsic micropores of material might serve the purpose of solvent extravasation from the adhered dye molecules [32].

The impact of the initial concentration of CR solution was subsequently investigated. As the initial dye concentration increased from 50 to 1000 ppm, the adsorption capacity of ZIF-9 increased accordingly, reaching saturation at 200 ppm with a CR uptake of 240.1 mg/g. Hence, the adsorption dynamic was indeed dependent on the initial concentration of the anionic dye. However, beyond 200 ppm, there was minimal change in adsorption efficiency, with a slight increase to 259.5 mg/g at 1000 ppm (Fig. 7). In other words, the observed improvement in the adsorption efficiency of ZIF-9 might be related to the concentration gradient, which provided the driving force for the mass transfer of CR molecules from the solution towards the surface of ZIF-9 per unit of time with increasing initial CR concentration up to a certain value, namely 200 ppm. This result suggested the adsorptive sites within the ZIF-9 network were no longer available, and the saturation state of CR adsorption was probably achieved.

These initial dye concentration-dependent trapping capacities were applied to investigate the adsorption kinetics of CR from aqueous solution onto the ZIF-9 surface, employing two typical isothermal adsorption models, namely Langmuir and Freundlich models (Fig. 8).

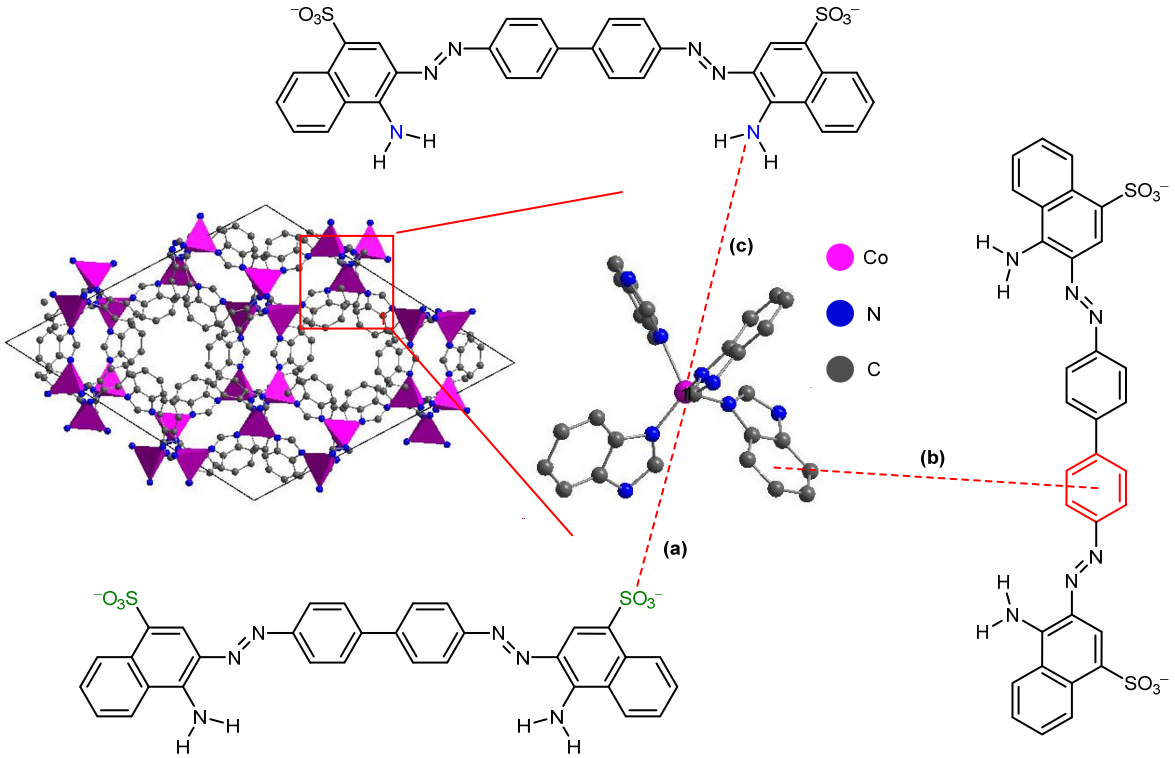

Fig 6. Plausible interactions of the ZIF-9 with CR: (a) electrostatic attraction, (b) π-π interaction, (c) coordination bond

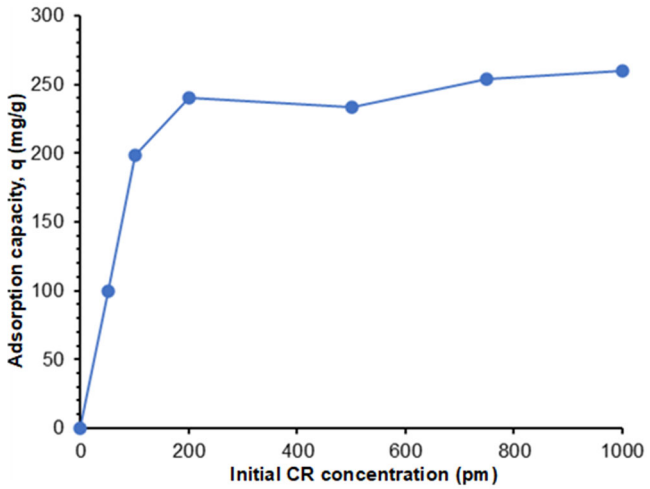

Fig 7. Adsorption capacity versus initial CR concentration (Experimental conditions: ZIF-9 10 mg, contact time 240 min)

The Freundlich isotherm displayed a lower determination coefficient ($R^2 = 0.7591$). Meanwhile, the Langmuir model exhibited a higher determination coefficient ($R^2 = 0.9956$), making it more appropriate for describing the capturing process. The adsorption of CR onto the ZIF-9 surface might occur at adsorption sites until reaching saturation, with minimal interactions between the adsorbed dye molecules and even neighboring sites. The Langmuir model also assumes that the adsorption is monolayer and is dependent on active sites on the adsorbent surface with constant and uniform energy [37]. The Freundlich isothermal adsorption model is an empirical model used to describe non-homogeneous but not limited to multi-layer adsorption in which the solid surface is uneven [38]. Furthermore, the maximum CR uptake amount deriving from the Langmuir equation was calculated to be 248.2 mg/g, which was closely equal to the experimental result of 240.1 mg/g. The CR uptake exhibited superiority over the previous study, which could be attributed to medium and large-sized slit-like pores deriving from the irregular distribution of the stacked ZIF-9 layers and particles, affording comparable CR dye capture. The CR adsorption process might be involved in the even distribution of CR molecules adhered onto the binding sites *via* electrostatic attractions, π-π stacking and coordination bonding, forming a single layer on the surface of ZIF-9 (Fig. 6).

To study the effect of pH on CR adsorption by ZIF-9, experiments with the pH range from 4 to 11 were conducted and the adsorption capacity of CR was recorded and shown in Fig. 9. The adsorption capacity increased as the pH increased from 4.0 to 7.0, with the highest adsorption capacity at pH = 7.0 being 200.14 mg/g. It can be explained that in an acidic environment, the ionization of Na^+ was inhibited by a high number of H^+ ions, which decreased the CR adsorption uptake [39]. When the initial pH value is in the range between 7.0 and 10.0, CR's high adsorption capacities remain at approximately 200 mg/g. However, as the initial pH of the solution further increased to 11.0, the CR adsorption capacity of ZIF-9 decreased to approximately 150 mg/g. The main reason could be that a great amount of OH^- ion in the solution would compete with CR for active sites in the basic environment [40].

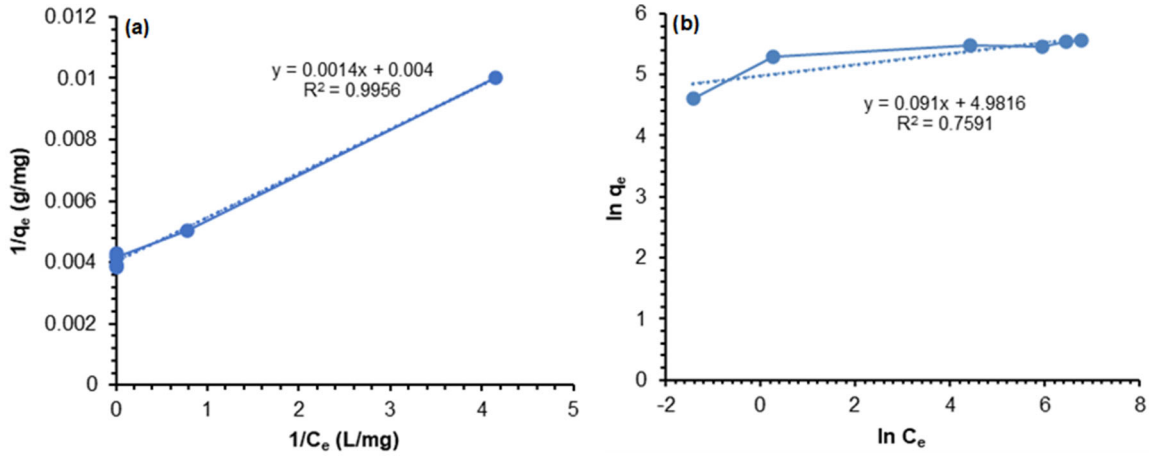

Fig 8. (a) Langmuir adsorption and (b) Freundlich adsorption isotherm of CR adsorbing on ZIF-9

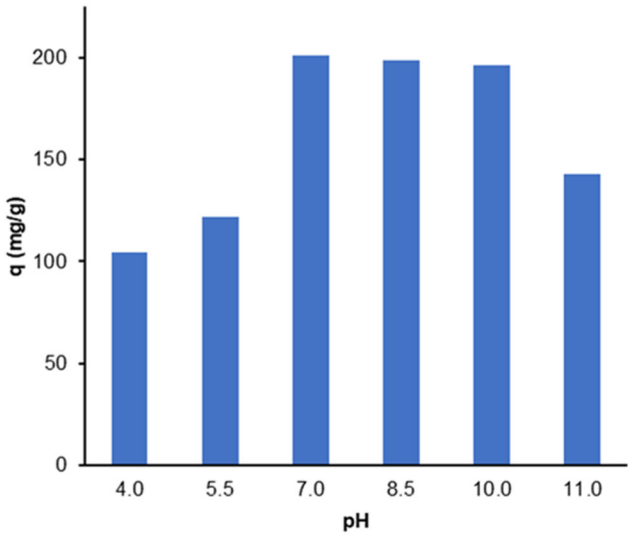

Fig 9. CR uptake versus initial pH (Experimental conditions: ZIF-9 10 mg, contact time 240 min, initial pH was modified by adding HCl and NaOH solutions)

The ZIF-9 material was employed for three reused cycles of adsorption experiments to investigate the reusability (Fig. 10). After achieving adsorption equilibrium in each cycle, the adsorbent was collected by centrifugation, washed with ethanol, dried at 120 °C, and reused for the next cycle. The adsorption capacity of ZIF-9 decreased over each generation cycle, from 201.14 mg/g in the first cycle to 125.70 mg/g in the third cycle, which could be attributed to several factors. Firstly, some CR molecules were tightly adsorbed on the adsorbent surface and could not be desorbed completely, resulting in a lower number of active sites after each reuse cycle [41]. Second, the repeated exposure of ZIF-9 to CR molecules could cause physical or chemical changes on the surface of the material [42].

The CR adsorption capacity of mechanochemically synthesized ZIF-9 was evaluated and compared with previously reported adsorbents (Table 1). In particular, the adsorption process of MgO-graphene oxide, Fe-MIL-88NH$_2$, and UIO-66-TETA relied on electrostatic and π-π interaction, similar to the mechanism used by ZIF-9. It should be noted that the fabrication of those materials required many toxic chemicals, intensive energy, and complicated processes. In this study, ZIF-9 synthesis utilized a solvent-free mechanochemical pathway to overcome such disadvantages, providing a greener and more sustainable alternative. This environmentally friendly approach highlighted the potential of ZIF-9 for

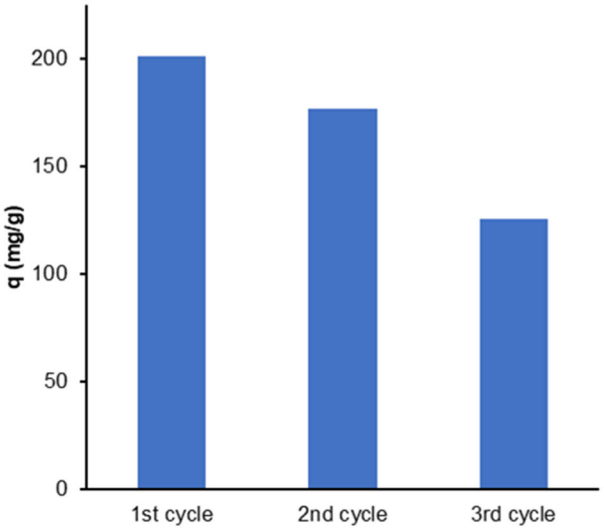

Fig 10. CR uptake versus number of cycles

Table 1. CR adsorption capacity of various adsorbents

Materials	Precursors	Synthesis method	Mechanism of adsorption	Adsorption capacity (mg/g)	Ref.
ZIF-9	Cobalt nitrate, benzimidazole, potassium carbonate	Mechanochemistry	Electrostatic interaction, π-π interaction, coordinated bond	248.14	This study
Fe-MIL-88NH$_2$	Ferric chloride, 2-amino-terephthalic acid, *N,N*-dimethylformamide	Solvothermal	Electrostatic interaction	175.00	[43]
Ag-Cu-CeO$_2$	Silver acetate, cerium nitrate, copper sulfate, cetyltrimethylammonium bromide	Co-precipitation	Electrostatic interaction, hydrogen bonding, coordinated bond	54.71	[44]
MgO-graphene oxide	Graphene oxide, magnesium acetate, ethylene glycol, ethanol, polyvinylpyrrolidone	Solvothermal	Electrostatic interaction, π-π interaction	237.00	[45]

Materials	Precursors	Synthesis method	Mechanism of adsorption	Adsorption capacity (mg/g)	Ref.
Cu-MOF	Copper chloride, methyl-1*H*-1,2,4-triazole-3-carboxylate, water	Hydrothermal	Electrostatic interaction, π-π interaction, van der Waals interaction	119.76	[46]
Melamine sponge/polyvinyl alcohol@UIO-66-TETA	Polyvinyl alcohol, zirconium tetrachloride, triethylenetetramine dimethylformamide, ethanol, glutaraldehyde, methanol, 2-aminoterephthalic acid	Solvothermal	Electrostatic interaction, π-π interaction, hydrogen interaction	303.95	[47]

practical application in removing emerging organic contaminants.

■ CONCLUSION

In summary, mechanochemical synthesis has proved to be a successful method for the preparation of ZIF-9 without the addition of any solvents during the synthesis phase. Compared to the liquid-based synthesis methods, the mechanochemical approach makes it possible to reduce the amount of solvent used, the temperature of the synthesis process (ambient temperature), and the reaction time, making the preparation process more sustainable. The results demonstrated the feasibility of the CR molecules adsorption, in which the dye molecules adhered on the external surface of ZIF-9, whose pore diameter is far smaller than the anionic dye. The adsorption kinetics and isotherm were characterized via the pseudo-second-order model and Langmuir adsorption model, respectively. This study offered theoretical knowledge on MOF preparation for the water purification application that only a high BET surface area could not guarantee high adsorption capacity. The as-prepared ZIF-9 proved to be a promising candidate for water purification.

■ ACKNOWLEDGMENTS

We acknowledge Ho Chi Minh City University of Technology (HCMUT), VNU-HCM for supporting this study.

■ CONFLICT OF INTEREST

The authors declare that they have no known competing financial interests or personal relationships that could have appeared to influence the work reported in this paper.

■ AUTHOR CONTRIBUTIONS

Khoa Dang Tran, Hoan Tuan Phan, Chi Thi Kim Nguyen, Bao Chi Nguyen conducted the experiment, processed data, drafted and edited the manuscript. Khoa Dang Nguyen, Ha Vu Le conceptualized, validated, reviewed and edited manuscript. All authors read and approved of the final manuscript.

■ REFERENCES

[1] Phan, H.T., Nguyen, K.D., Nguyen, H.H.M., Dao, N.T., Le, P.T.K., and Le, H.V., 2023, *Nata de coco* as an abundant bacterial cellulose resource to prepare aerogels for the removal of organic dyes in water, *Bioresour. Technol. Rep.*, 24, 101613.

[2] Ghorai, S., Sarkar, A.K., Panda, A.B., and Pal, S., 2013, Effective removal of Congo red dye from aqueous solution using modified xanthan gum/silica hybrid nanocomposite as adsorbent, *Bioresour. Technol.*, 144, 485–491.

[3] Siddiqui, S.I., Allehyani, E.S., Al-Harbi, S.A., Hasan, Z., Abomuti, M.A., Rajor, H.K., and Oh, S., 2023, Investigation of Congo red toxicity towards different living organisms: A review, *Processes*, 11 (3), 807.

[4] Lipskikh, O.I., Korotkova, E.I., Khristunova, Y.P., Barek, J., and Kratochvil, B., 2018, Sensors for voltammetric determination of food azo dyes - A critical review, *Electrochim. Acta*, 260, 974–985.

[5] Le, H.V., Dao, N.T., Bui, H.T., Kim Le, P.T., Le, K.A., Tuong Tran, A.T., Nguyen, K.D., Mai Nguyen, H.H., and Ho, P.H., 2023, Bacterial cellulose aerogels derived from pineapple peel waste for the adsorption of dyes, *ACS Omega*, 8 (37), 33412–33425.

[6] Hambisa, A.A., Regasa, M.B., Ejigu, H.G., and Senbeto, C.B., 2022, Adsorption studies of methyl orange dye removal from aqueous solution using Anchote peel-based agricultural waste adsorbent, *Appl. Water Sci.*, 13 (1), 24.

[7] Hikmah, N., Agustiningsih, D., Nuryono, N., and Kunarti, E.S., 2021, Preparation of iron-doped SiO_2/TiO_2 using silica from sugarcane bagasse ash for visible light degradation of Congo red, *Indones. J. Chem.*, 22 (2), 402–412.

[8] Fakhri, F.H., and Ahmed, L.M., 2019, Incorporation CdS with ZnS as composite and using in photo-decolorization of Congo red dye, *Indones. J. Chem.*, 19 (4), 936–943.

[9] Wong, S., Abd Ghafar, N., Ngadi, N., Razmi, F.A., Inuwa, I.M., Mat, R., and Saidina Amin, N.A., 2020, Effective removal of anionic textile dyes using adsorbent synthesized from coffee waste, *Sci. Rep.*, 10 (1), 2928.

[10] Lafi, R., Montasser, I., and Hafiane, A., 2019, Adsorption of Congo red dye from aqueous solutions by prepared activated carbon with oxygen-containing functional groups and its regeneration, *Adsorpt. Sci. Technol.*, 37 (1-2), 160–181.

[11] Chatterjee, S., Guha, N., Krishnan, S., Singh, A.K., Mathur, P., and Rai, D.K., 2020, Selective and recyclable Congo red dye adsorption by spherical Fe_3O_4 nanoparticles functionalized with 1,2,4,5-benzenetetracarboxylic Acid, *Sci. Rep.*, 10 (1), 111.

[12] Stjepanović, M., Velić, N., Galić, A., Kosović, I., Jakovljević, T., and Habuda-Stanić, M., 2021, From waste to biosorbent: Removal of Congo red from water by waste wood biomass, *Water*, 13 (3), 279.

[13] Lu, W., Wei, Z., Gu, Z.Y., Liu, T.F., Park, J., Park, J., Tian, J., Zhang, M., Zhang, Q., Gentle III, T., Bosch, M., and Zhou, H.C., 2014, Tuning the structure and function of metal–organic frameworks via linker design, *Chem. Soc. Rev.*, 43 (16), 5561–5593.

[14] Nguyen, K.D., Vo, N.T., Le, K.T.M., Ho, K.V., Phan, N.T.S., Ho, P.H., and Le, H.V., 2023, Defect-engineered metal–organic frameworks (MOF-808) towards the improved adsorptive removal of organic dyes and chromium (VI) species from water, *New J. Chem.*, 47 (13), 6433–6447.

[15] Park, K.S., Ni, Z., Côté, A.P., Choi, J.Y., Huang, R., Uribe-Romo, F.J., Chae, H.K., O'Keeffe, M., and Yaghi, O.M., 2006, Exceptional chemical and thermal stability of zeolitic imidazolate frameworks, *Proc. Natl. Acad. Sci. U. S. A.*, 103 (27), 10186–10191.

[16] Duong, A.T.A., Nguyen, H.V., Tran, M.V., Ngo, Q.N., Luu, L.C., Doan, T.L.H., Nguyen, H.N., and Nguyen, M.V., 2023, Influence of ZIF-9 and ZIF-12 structure on the formation of a series of new Co/N-doped porous carbon composites as anode electrodes for high-performance lithium-ion batteries, *RSC Adv.*, 13 (25), 17370–17383.

[17] Öztürk, Z., Hofmann, J., Lutz, M., Mazaj, M., Logar, N.Z., and Weckhuysen, B., 2015, Controlled synthesis of phase-pure zeolitic imidazolate framework Co-ZIF-9, *Eur. J. Inorg. Chem.*, 2015 (9), 1625–1630.

[18] Noguera-Díaz, A., Villarroel-Rocha, J., Ting, V.P., Bimbo, N., Sapag, K., and Mays, T.J., 2019, Flexible ZIFs: Probing guest-induced flexibility with CO_2, N_2 and Ar adsorption, *J. Chem. Technol. Biotechnol.*, 94 (12), 3787–3792.

[19] Dai, J., Xiao, S., Liu, J., He, J., Lei, J., and Wang, L., 2017, Fabrication of ZIF-9@super-macroporous microsphere for adsorptive removal of Congo red from water, *RSC Adv.*, 7 (11), 6288–6296.

[20] Dapson, R.W., 2018, Amyloid from a histochemical perspective. A review of the structure, properties and types of amyloid, and a proposed staining mechanism for Congo red staining, *Biotech. Histochem.*, 93 (8), 543–556.

[21] Do, J.L., and Friščić, T., 2017, Mechanochemistry: A force of synthesis, *ACS Cent. Sci.*, 3 (1), 13–19.

[22] Prochowicz, D., Sokołowski, K., Justyniak, I., Kornowicz, A., Fairen-Jimenez, D., Friščić, T., and Lewiński, J., 2015, A mechanochemical strategy for IRMOF assembly based on pre-designed oxo-zinc precursors, *Chem. Commun.*, 51 (19), 4032–4035.

[23] Beldon, P.J., Fábián, L., Stein, R.S., Thirumurugan, A., Cheetham, A.K., and Friščić, T., 2010, Rapid

room-temperature synthesis of zeolitic imidazolate frameworks by using mechanochemistry, *Angew. Chem. Int. Ed.*, 49 (50), 9640–9643.

[24] Užarević, K., Wang, T.C., Moon, S.Y., Fidelli, A.M., Hupp, J.T., Farha, O.K., and Friščić, T., 2016, Mechanochemical and solvent-free assembly of zirconium-based metal–organic frameworks, *Chem. Commun.*, 52 (10), 2133–2136.

[25] Revellame, E.D., Fortela, D.L., Sharp, W., Hernandez, R., and Zappi, M.E., 2020, Adsorption kinetic modeling using pseudo-first order and pseudo-second order rate laws: A review, *Cleaner Eng. Technol.*, 1, 100032.

[26] Ho, Y.S., and McKay, G., 1999, Pseudo-second order model for sorption processes, *Process Biochem.*, 34 (5), 451–465.

[27] Langmuir, I., 1918, The adsorption of gases on plane surfaces of glass, mica and platinum, *J. Am. Chem. Soc.*, 40 (9), 1361–1403.

[28] He, H., Li, R., Yang, Z., Chai, L., Jin, L., Alhassan, S.I., Ren, L., Wang, H., and Huang, L., 2021, Preparation of MOFs and MOFs derived materials and their catalytic application in air pollution: A review, *Catal. Today.*, 375, 10–29.

[29] Tuo, Y., Liu, W., Chen, C., Lu, Q., Zhou, Y., and Zhang, J., 2021, Constructing $RuCoO_x$/NC nanosheets with low crystallinity within ZIF-9 as bifunctional catalysts for highly efficient overall water splitting, *Chem. Asian J.*, 16 (17), 2511–2519.

[30] Chen, W., Wang, C., Su, S., Wang, H., and Cai, D., 2021, Synthesis of ZIF-9(III)/Co LDH layered composite from ZIF-9(I) based on controllable phase transition for enhanced electrocatalytic oxygen evolution reaction, *Chem. Eng. J.*, 414, 128784.

[31] Lewis, D.W., Ruiz-Salvador, A.R., Gómez, A., Rodriguez-Albelo, L.M., Coudert, F.X., Slater, B., Cheetham, A.K., and Mellot-Draznieks, C., 2009, Zeolitic imidazole frameworks: Structural and energetics trends compared with their zeolite analogues, *CrystEngComm*, 11 (11), 2272–2276.

[32] Luan Tran, B., Chin, H.Y., Chang, B.K., and Chiang, A.S.T., 2019, Dye adsorption in ZIF-8: The importance of external surface area, *Microporous Mesoporous Mater.*, 277, 149–153.

[33] Xiao, G., Chen, W., Cai, Y., Zhang, S., Wang, D., and Cai, D., 2022, Facile synthesis of sulfate-intercalated CoFe LDH nanosheets derived from two-dimensional ZIF-9(III) for promoted oxygen evolution reaction, *Catalysts*, 12 (7), 688.

[34] Liu, J., Liu, C., and Huang, A., 2020, Co-based zeolitic imidazolate framework ZIF-9 membranes prepared on α-Al_2O_3 tubes through covalent modification for hydrogen separation, *Int. J. Hydrogen Energy*, 45 (1), 703–711.

[35] Aboua, K.N., Yobouet, Y.A., Yao, K.B., Goné, D.L., and Trokourey, A., 2015, Investigation of dye adsorption onto activated carbon from the shells of Macoré fruit, *J. Environ. Manage.*, 156, 10–14.

[36] Kiwaan, H.A., Sh. Mohamed, F., El-Bindary, A.A., El-Ghamaz, N.A., Abo-Yassin, H.R., and El-Bindary, M.A., 2021, Synthesis, identification and application of metal organic framework for removal of industrial cationic dyes, *J. Mol. Liq.*, 342, 117435.

[37] Song, X., Zhang, Y., Yan, C., Jiang, W., and Chang, C., 2013, The Langmuir monolayer adsorption model of organic matter into effective pores in activated carbon, *J. Colloid Interface Sci.*, 389 (1), 213–219.

[38] Kalam, S., Abu-Khamsin, S.A., Kamal, M.S., and Patil, S., 2021, Surfactant adsorption isotherms: A review, *ACS Omega*, 6 (48), 32342–32348.

[39] Eltaweil, A.S., Elshishini, H.M., Ghatass, Z.F., and Elsubruiti, G.M., 2021, Ultra-high adsorption capacity and selective removal of Congo red over aminated graphene oxide modified Mn-doped UiO-66 MOF, *Powder Technol.*, 379, 407–416.

[40] Tan, Y., Huang, W., Lei, Q., Huang, S., Yang, K., Chen, X., and Li, D., 2023, Insight into the adsorption of magnetic microspheres with large mesopores: Tailoring mesoporous structure and ethylenediamine functionalization for ultrahigh Congo red removal, *Sep. Purif. Technol.*, 311, 123265.

[41] Hu, N., Yu, J., Hou, L., Shi, C., Li, K., Hang, F., and Xie, C., 2023, Amine-functionalized MOF-derived

carbon materials for efficient removal of Congo red dye from aqueous solutions: Simulation and adsorption studies, *RSC Adv.*, 13 (1), 1–13.

[42] Daffalla, S., Taha, A., Da'na, E., and El-Aassar, M.R., 2024, Sustainable banana-waste-derived biosorbent for Congo red removal from aqueous solutions: Kinetics, equilibrium, and breakthrough studies, *Water*, 16 (10), 1449.

[43] Fu, Q., Lou, J., Zhang, R., Peng, L., Zhou, S., Yan, W., Mo, C., and Luo, J., 2021, Highly effective and fast removal of Congo red from wastewater with metal-organic framework Fe-MIL-88NH_2, *J. Solid State Chem.*, 294, 121836.

[44] Semwal, N., Mahar, D., Chatti, M., Dandapat, A., and Chandra Arya, M., 2023, Adsorptive removal of Congo red dye from its aqueous solution by Ag-Cu-CeO_2 nanocomposites: Adsorption kinetics, isotherms, and thermodynamics, *Heliyon*, 9 (11), e22027.

[45] Xu, J., Xu, D., Zhu, B., Cheng, B., and Jiang, C., 2018, Adsorptive removal of an anionic dye Congo red by flower-like hierarchical magnesium oxide (MgO)-graphene oxide composite microspheres, *Appl. Surf. Sci.*, 435, 1136–1142.

[46] Wang, Y., Ren, D., Ye, J., Li, Q., Yang, D., Wu, D., Zhao, J., and Zou, Y., 2024, Highly efficient and targeted adsorption of Congo Red in a novel cationic copper-organic framework with three-dimensional cages, *Sep. Purif. Technol.*, 329, 125149.

[47] Zhao, H., Li, T., Zhang, M., Peng, X., Xu, C., Su, J., Yang, Z., Liu, X., Sun, G., and Cui, Y., 2024, Enhanced removal of Pb^{2+} and Congo red from aqueous solutions using hierarchically porous melamine sponge/polyvinyl alcohol/Zr-MOF composites, *J. Environ. Chem. Eng.*, 12 (2), 112361.